Simulation of Semiconductor Processes and Devices 2016
Edited by E. Bär, J. Lorenz, and P. Pichler

Atomistic Simulation of Nanodevices

(Invited Paper)

Mathieu Luisier*, Reto Rhyner†, Aron Szabo*, and Andreas Pedersen*
*Integrated Systems Laboratory, ETH Zürich, CH-8092 Zürich, Switzerland
† Synopsys Switzerland LLC, CH-8050 Zürich, Switzerland

***Abstract*—As the dimensions of electronic devices, especially transistors, are getting smaller and smaller, novel modeling approaches must be developed to reveal the physics and predict the performance of not-yet-fabricated ultra-scaled components. In this paper the basic requirements to simulate nanoscale devices are first reviewed before introducing a hierarchical quantum transport approach going from empirical to *ab-initio* models. It is illustrated with three examples, a Si nanowire transistor treated within nearest-neighbor tight-binding (TB), a 2-D logic switch based on transition metal dichalcogenides and investigated with an hybrid scheme combining the advantages of TB and density-functional theory, and finally a silver nano-filament explored at the first-principles level. The importance of dissipative effects such as electron-phonon scattering is discussed in all applications.**

I. Introduction

At the heart of laptops, tablets, or cell phones sit integrated circuits, lithium ion batteries, and memory cells that ensure the proper functionality of these modern electronic devices. By further diving into these hardware components, one may find integrated circuits relying on nanoscale logic switches, in most cases FinFETs, cathodes and anodes with high power and energy densities due to the presence of porous nano-particles, or ultra-short metal-insulator-metal junctions enabling a non-volatile storage of digital information. Besides reduced dimensions the mentioned nanostructures share other peculiar features: their active region is usually made of a countable number of atoms and their behavior is strongly influenced by quantum mechanical effects. As a consequence and contrary to the recent past, standard recipes, intuition, and extrapolation from previous generations might not be sufficient anymore to design novel nanoelectronic devices with enhanced performance and higher complexity.

The experimental work can be greatly enhanced by adding a modeling activity to support the initial design process and shed light on the mechanisms that determine the properties of fabricated samples. If a suitable technology computer aided design tool (TCAD) is available, less trial-and-error iterations are needed before a successful prototype is demonstrated. This is particularly true at the nanoscale, where the costs of production are consequent and the manufacturing cycles relatively long. To be useful to a nano-device engineer, a TCAD tool should provide measurable data that can be directly compared to experiments and give access to internal quantities whose knowledge is essential to understand the behavior of the considered systems. This includes for example insights into the underlying atomic structure, the magnitude of the electron/hole currents induced by the application of external voltages, the carrier trajectories inside the active region, or the distribution of the lattice temperature. The right physical models should be implemented in the chosen TCAD framework to make such detailed analyses possible.

Since (semi-)classical theories such as drift-diffusion or the Boltzmann Transport Equation fails at incorporating the atomistic granularity of simulation domains as well as quantum mechanical effects, they should be replaced by more advanced techniques that offer the desired level of accuracy. At the nanometer scale a direct solution of the Schrödinger equation imposes itself to account for atomistic quantum transport phenomena. This can be achieved with the well-established Non-equilibrium Green's Function (NEGF) formalism, which will be briefly summarized here in Section II and illustrated with three different examples in Section III.

II. Simulation Approach

To determine the transport properties of nanoscale devices, open boundary conditions (OBCs) should be introduced into the Schrödinger equation in order to enable the injection of fermions and bosons into the simulated region. If this is done in the framework of NEGF [1] the generic equations for fermions are the following

$$\left(E - H(k) - \Sigma^R(k,E)\right) \cdot G^R(k,E) = I \quad (1)$$

$$G^{\gtrless}(k,E) = G^R(k,E) \cdot \Sigma^{\gtrless}(k,E) \cdot G^A(k,E), \quad (2)$$

$$\Sigma^{\gtrless,R}(E,k) = \Sigma^{\gtrless,RB}(E,k) + \Sigma^{\gtrless,RS}(E,k). \quad (3)$$

Similar equations can be derived for phonons [2] and photons. In Eqs. (1) and (2), the unknowns are the retarded/advanced $G^{R/A}(k,E)$ and lesser/greater $G^{\gtrless}(k,E)$ Green's functions at energy E and momentum k. They are full matrices of size $N_A \times N_B$ where N_A is the number of discretization points in the simulation domain and N_B the number of basis components describing each of them. The momentum (k) dependence arises from the modeling of the directions that are assumed periodic. The diagonal matrix E contains the electron/hole energy, the usually block tri-diagonal matrix $H(k)$ is the device Hamiltonian, while the open boundary conditions are cast into the self-energy matrices $\Sigma^{R,\gtrless B}(k,E)$ and the scattering mechanisms into $\Sigma^{R,\gtrless S}(k,E)$. The key ingredients in Eqs. (1) and (2) are the Hamiltonian $H(k)$ that can be expressed in various atomistic basis sets, as will be discussed in Section III, and the choice of the interactions that are integrated into $\Sigma^{\gtrless,RS}(k,E)$.

978-1-5090-0818-6/16/$31.00 © 2016 IEEE

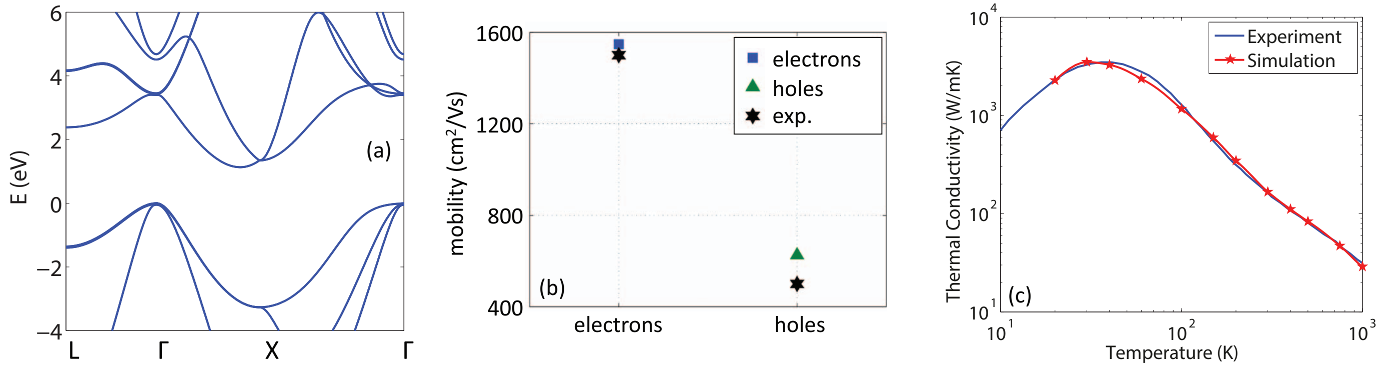

Fig. 1. (a) Si bulk bandstructure as computed with the nearest-neighbor tight-binding parameters of Ref. [9]. (b) Electron and hole mobility of bulk Si. The square and triangle refer to calculations performed with the "dR/dL" method [10] in the presence of electron-phonon scattering, the stars to experimental data. (c) Lattice thermal conductivity of bulk Si as obtained from phonon quantum transport simulations including anharmonic phonon phonon scattering (red line with symbols) and from experiments (blue line) [11].

A. Ballistic Transport

The NEGF formalism is best-suited for transport situations where scattering should be accounted for. In the ballistic limit, Eq. (1) can be reformulated into a Wave Function problem known as Quantum Transmitting Boundary Method (QTBM) that produces exactly the same results as NEGF, but faster since it takes the form of a sparse linear system of equations "Ax=b" [3], [4]

$$\underbrace{\left(E - H(k) - \Sigma^{RB}(E,k)\right)}_{A} \cdot \underbrace{C(E,k)}_{x} = \underbrace{Inj(E,k)}_{b}. \quad (4)$$

In Eq. (4) the injection vector $Inj(E,k)$ is also part of the OBCs and the unknowns are the expansion coefficients $C(E,k)$. Direct sparse linear solvers, sequential or parallel, can be utilized to handle the "Ax=b" system in Eq. (4).

B. Dissipative Transport: Electron-Phonon Scattering

As soon as scattering is turned on, the NEGF formalism should be used because it lends itself naturally to this kind of physical problems. In case of electron-phonon scattering, the lesser scattering self-energy can be formulated as

$$\begin{aligned}\Sigma^{<S}(k,E) \quad \propto \quad & \sum_{\omega} \int \frac{dq}{2\pi} V(\omega,q) \\ & \nabla H \left(n_\omega G^<(k-q,E+\hbar\omega) + \right. \\ & \left. (n_\omega + 1) G^<(k-q,E-\hbar\omega)\right) \nabla H \quad (5)\end{aligned}$$

The expression for $\Sigma^{>S}(k,E)$ and $\Sigma^{RS}(k,E)$ can be found in Ref. [5]. The phonon frequencies ω and modes μ enter this equation, either directly or through the form factor $V(\omega,q)$ that is a function of both of them and through the phonon distribution function n_ω (Bose-Einstein). Here, it is assumed that the phonon population remains in equilibrium with its environment, but it can be driven out-of-equilibrium by solving the corresponding phonon Green's functions and phonon-electron scattering self-energy [6]. This gives rise to self-heating effects and the formation of local hot spots.

Since $\Sigma^{<S}(k,E)$ in Eq. (5) depends on the Green's Function and vice-versa, these quantities must be iteratively computed in the so-called self-consistent Born approximation till convergence is reached. It is very convenient to solve Eqs. (1) and (2) with a recursive Green's Function (RGF) algorithm [7]. Finally, regardless of the transport regime, ballistic or dissipative, Eqs. (1) and (2) or Eq. (4) must be evaluated at each possible E and k to obtain the current and charge density of the considered devices. The charge is then self-consistently coupled to the electrostatic potential through Poisson's equation expressed on a finite element grid.

III. Results

Three applications have been selected to highlight the benefits of atomistic quantum transport simulations. Each of them relies on a different device configuration (Si nanowire, 2-D semiconductor, Ag nano-filament) and on a different modeling approach (tight-binding, Wannier functions, *ab-initio* basis).

A. Tight-Binding

Empirical nearest-neighbor tight-binding models, as proposed by Slater and Koster [8], allow to account for full bandstructures at low computational costs, while still capturing every single atom constituting the investigated device structures. An example with bulk Si is given in Fig. 1(a), where the $sp^3d^5s^*$ parameterization of Ref. [9] has been used. By turning on electron-phonon scattering, the bulk electron and hole mobility of Si can be obtained, as shown in Fig. 1(b). This requires either solving the linearized Boltzmann Transport Equation or applying the "dR/dL" method and extracting the resistance of samples with various lengths [10]. The results of both approaches agree very well with available experimental data, especially for electrons. However, with the chosen parameters the hole mobility tends to be overestimated by about 100 cm^2/Vs, which remains acceptable in most applications.

The counterpart of tight-binding for phonons is the so-called valence-force-field (VFF) method that produces the oscillation frequencies and amplitudes of a given crystal based on a limited number of input parameters, typically between 2 and

Simulation of Semiconductor Processes and Devices 2016
Edited by E. Bär, J. Lorenz, and P. Pichler

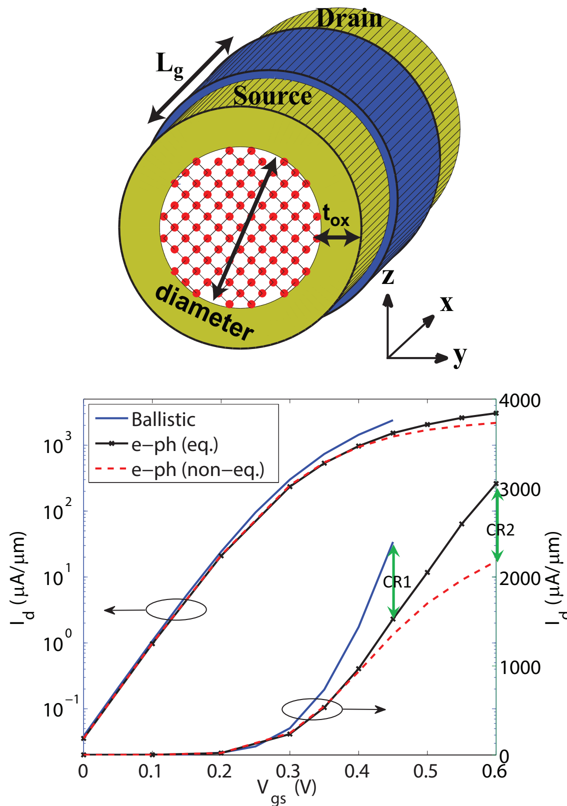

Fig. 2. (top) Schematic view of an ultrascaled Si nanowire transistor with a gate-all-around contact of length L_g=5 nm, a semiconductor diameter d=3 nm, and an oxide thickness t_{ox}=3 nm with a relative permittivity ϵ_R=20. Transport occurs along the x=<100> crystal axis. (bottom) Transfer characteristics I_d-V_{gs} at V_{ds}=0.6 V of the nanowire FET above. The blue line represents the ballistic limit of transport, the black one with crosses the case where electron-phonon scattering is included, but phonons remain in equilibrium with their surrounding, and the dashed orange curve the situation where both electron and phonon populations are driven out-of-equilibrium. The quantities CR1 and CR2 indicate the current reduction caused by first going beyond ballistic transport and then accounting for non-equilibrium phonons, respectively.

7 when Coulomb interactions are considered. VFF can deliver the phonon data needed in mobility calculations. It can also be used to evaluate the lattice thermal conductivity of materials, as demonstrated in Fig. 1(c) for bulk Si. These results have been obtained in the presence of anharmonic phonon scattering [11].

Both tight-binding and VFF can be extended to nanostructures, where the parameters are assumed to be the same as in bulk. As an example, the n-type ultra-scaled Si gate-all-around nanowire field-effect transistor (FET) in Fig. 2 has been simulated. Such logic switches are often seen as promising candidates at the end of the roadmap for semiconductors since they represent the most natural evolution of FinFETs. The here plotted structure has a gate length of 5 nm only and a diameter of 3nm. Its transfer characteristics are reported in Fig. 2, starting from the ballistic limit of transport, then with the inclusion of equilibrium phonon interactions, and finally with an out-of-equilibrium phonon population.

Despite the very short gate contact electron-phonon scattering still plays a major role. Electrons interacting with phonons may not only loose energy, but also change their direction of propagation. The resulting backscattering process induces a current reduction labeled CR1 in Fig. 2. A second current decrease (CR2) occurs when the phonon population is allowed to vary, e.g. when electrons transfer part of their energy to the lattice. The additional crystal vibrations have the possibility to interact with electrons close to the source extension of the transistor, which further reduces the current magnitude [6]. These findings indicate that no matter how short a Si transistor becomes electron-phonon scattering should still be fully accounted for to ensure accurate performance predictions.

B. Maximally Localized Wannier Functions

The main limitation of tight-binding and VFF is their empirical character: no component can be simulated before a parameter set has been established for its constituent materials. This is very challenging when a large material space should be explored for which no parameter has been created, as in the case of 2-D semiconductors. Since the first experimental demonstration of a single-layer MoS_2 transistor [12] the scientific interest for 2-D materials has not stopped growing, also from a modeling point of view [13]. Based on simple geometrical arguments it can be estimated that there exist more than 6000 2-D crystals. Not all of them are stable, but several thousands tight-binding and VFF parameter sets should still be prepared to study all relevant materials and compare them with each other.

Instead of tight-binding the Hamiltonian matrix in Eq. (1) could be directly expressed in an *ab-initio* basis such as density-functional theory (DFT) [15], which avoids any tedious parameterization, but is computationally much more intensive. As an alternative an intermediate scheme based on maximally localized Wannier functions (MLWFs) [14] is presented here. It can be seen as a first step towards first-principles devices simulations. The general idea is depicted in Fig. 3. It consists in identifying a small unit cell that is representative for the entire crystal structure of interest, computing its bandstructure with a plane-wave DFT code such as VASP [16] or Quantum ESPRESSO [17], and transforming the results into a set of MLWFs with the Wannier90 tool [18]. No approximation is involved in this procedure since a unitary transformation is performed. The only difference between the original plane-wave and final localized basis is that the latter only reproduces a sub-set of the full bandstructure, namely the sub-bands that matter in transport calculations. The MLWF-based Hamiltonian operator corresponding to the selected unit cell is then constructed and up-scaled to describe the entire simulation domain. It becomes a block-tridiagonal matrix similar to the tight-binding one, with beyond nearest-neighbor connections, but still ideal for quantum transport simulations.

This approach has been tested with the single-gate single-layer MoS_2 transistor in Fig. 4 that has a gate length of 10.7 nm. Its electronic structure as calculated with VASP [16] and the PBE exchange-correlation functional [19] is first shown and compared to the results obtained after a transformation

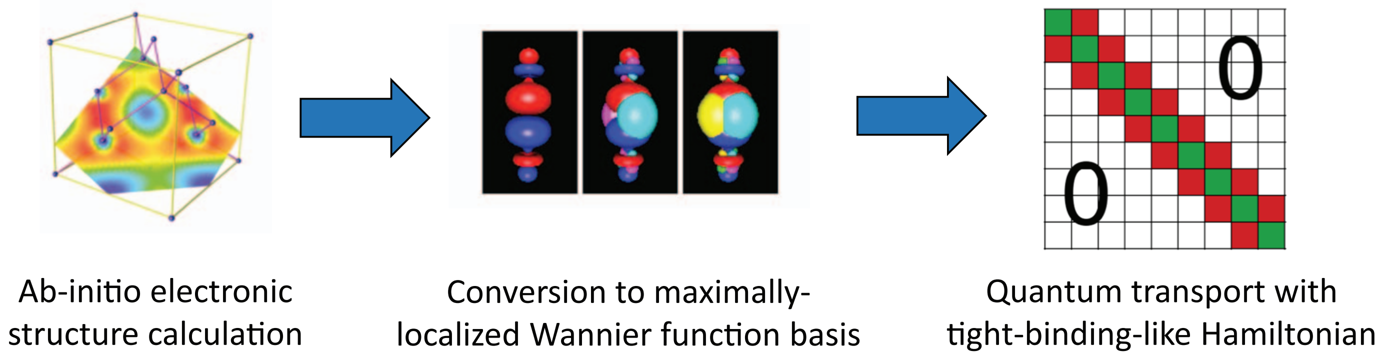

Fig. 3. Coupling scheme between density-functional theory, e.g. VASP [16] or Quantum ESPRESSO [17] and quantum transport calculations through the transformation of the produced plane-wave outputs into a set of maximally localized Wannier functions. The Wannier90 tool is used for that purpose [18]. This process results in a tight-binding-like Hamiltonian matrix with beyond nearest-neighbor connections.

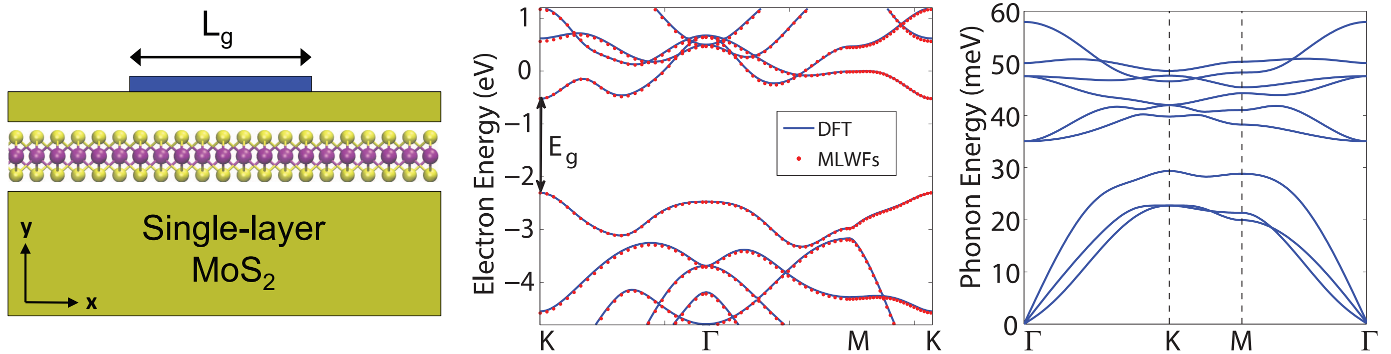

Fig. 4. (left) Schematic view of a single-gate transistor with a monolayer of MoS_2 as active region, L_g=10.7 nm, and an equivalent oxide thickness EOT=0.58 nm. (center) Comparison between the bandstructure of single-layer MoS_2 as calculated with a plane-wave DFT tool [16] and PBE functional [19] (solid blue lines) and with a quantum transport solver after a unitary transformation into MLWFs (red dots). (right) Phonon bandstructure of single-layer MoS_2 based on density-functional perturbation theory (DFPT) [21]

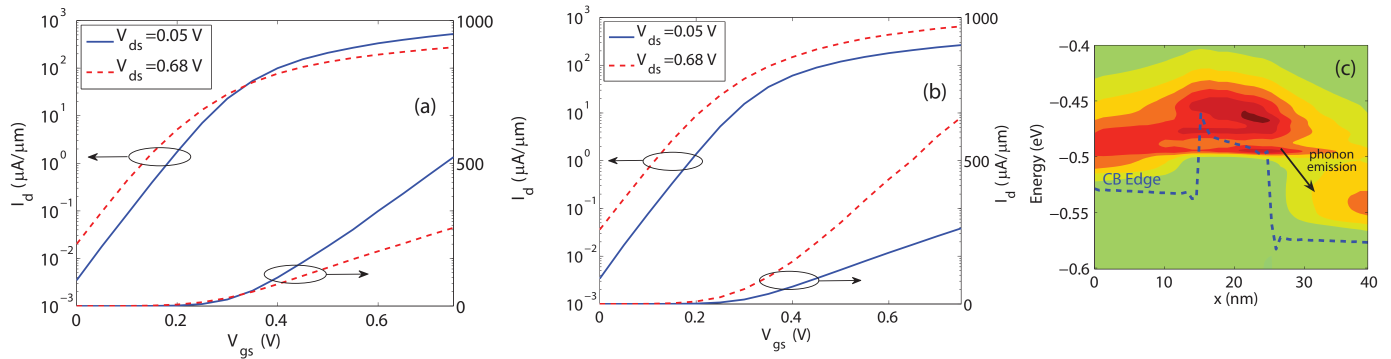

Fig. 5. (a) Ballistic transfer characteristics of the single-layer MoS_2 transistor in Fig. 4 at V_{ds}=0.05 V (solid blue line) and 0.68 V (dashed red line). (b) Same as (a), but in the presence of electron-phonon scattering. (c) Spectral current of the same transistor as before showing the band coupling induced by phonon emission. Red indicates high current concentrations, green no current, the dashed blue line refers to the conduction band edge.

into a MLWF basis with five d-like (three p-like) orbitals per Mo (S) atom. A very good agreement can be observed, although small discrepancies originating from the truncation of long-range interactions are present.

The ballistic transfer characteristics I_d-V_{gs} of this device at V_{ds}=0.05 and 0.68 V are presented in Fig. 5(a). A negative differential resistance (NDR) behavior can be noticed, i.e. the current at high V_{ds} is smaller than at low V_{ds}. It can be demonstrated that this is an artifact of the ballistic limit of transport where sub-bands with a limited energy width cannot be transmitted from source to drain [20]. By turning on electron-phonon scattering as in Eq. (5) the NDR disappears because phonon emissions and absorptions connect independent sub-bands that would otherwise not contribute to transport. This

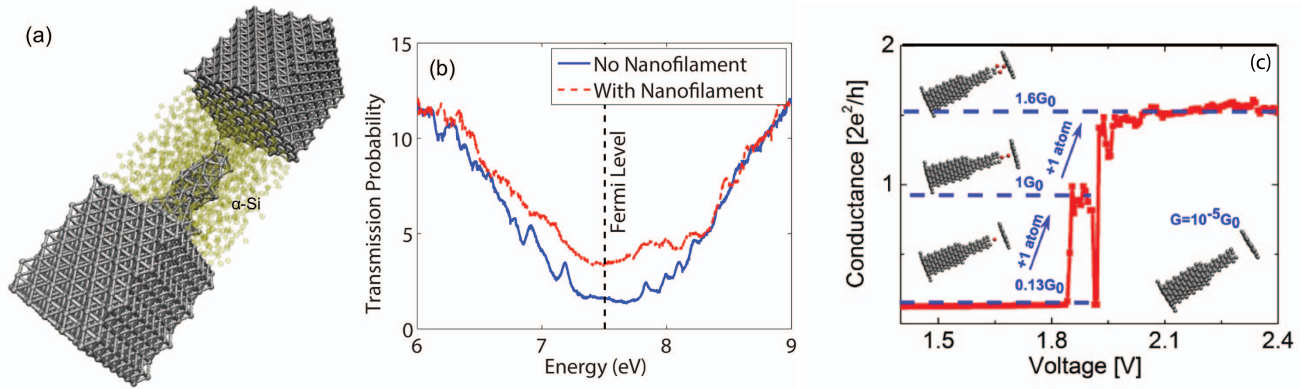

Fig. 6. (a) Realistic nano-filament structure composed of 4714 atoms. The gray dots refer to Ag atoms, the transparent yellow ones to Si. The latter form an amorphous Si (aSi) layer. The nano-filament is embedded between two metallic plates. (b) Transmission probability through the metal-aSi-metal structure in (a) with (dashed red line) and without (blue line) the Ag nano-filament inbetween. The position of the equilibrium Fermi level is indicated. A fully *ab-initio* quantum transport approach has been used to compute these curves. (c) Simulated (dashed blue curves) and measured (solid red line) conductance through an Ag nano-filament in terms of the conductance quantum G_0=7.74e-5 S as a function of the applied voltage [23]. The insets represent the atomic configuration corresponding to each conductance level, starting from the OFF-state (G=1e-5 G_0).

is confirmed in Fig. 5(b-c). Note that solving Eq. (5) in the present case requires the derivatives of the Hamiltonian matrix $H(k)$ in the MLWF basis with respect to the atom coordinates and the phonon modes and frequencies. While the former can be produced by Wannier90, the latter result from density-functional perturbation theory calculations [21]. The phonon bandstructure of single-layer MoS_2 is reported in Fig. 4.

C. Ab-initio Model

The last application deals with a memristor cell [22] based on the conductive bridging (CB) technology where an Ag nano-filament grows between two metallic plates, either connecting them (low resistance state: logic 1) or keeping them separated (high resistance state: logic 0). The CB memristor concept is illustrated in Fig. 6(a). Such a structure has been recently placed in the middle of a plasmonic cavity to form an optical switch [23]. The transition from the high to the low resistance state of the central memristor usually depends on the displacement of few Ag atoms, but at first it was not clear how many. This is exactly the kind of questions that atomistic device simulations can address.

The schemes that have been proposed so far, nearest-neighbor tight-binding and maximally localized Wannier functions, are not suitable to simulate metallic nano-filaments composed of several thousands atoms as in Fig. 6(a). First, the strong localization of the Löwding orbitals in tight-binding are not really compatible with the presence of delocalized states as in metals. Secondly, the transformation from plane-waves to MLWFs is limited to relatively small atomic systems and becomes computationally too intensive when the atom count exceeds several thousands. As a consequence, a full DFT quantum transport approach is needed to take care of the structure in Fig. 6(a) [24].

This can be done by coupling a DFT package working with a localized basis, e.g. SIESTA and its linear combination of atomic orbitals [25] or CP2K and its contracted Gaussian orbitals [26], and a NEGF solver. Here, it has been decided to transfer the Hamiltonian and overall matrices produced by CP2K to our in-house quantum transport code [4]. The developed work flow is shown in Fig. 7 and explained in great details in Ref. [27]. Basically, the same simulation framework as for tight-binding and MLWF can be used, except that more powerful numerical algorithms must be implemented to keep the computational burden manageable.

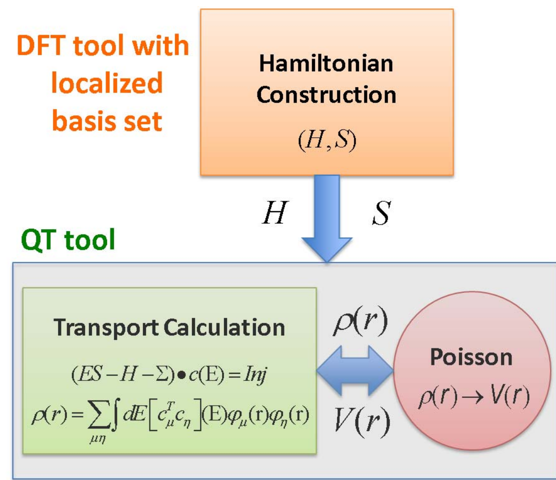

Fig. 7. Coupling scheme between a DFT solver relying on a non-orthogonal, but localized basis set, e.g. SIESTA [25] or CP2K [26] and a quantum transport tool importing the prepared Hamiltonian H and overlap S matrices and performing device simulations with them.

Simulation results can be found in Fig. 7(b-c). In the first sub-plot, the energy-resolved transmission probability between two metallic plates separated by an amorphous Si matrix is shown, once without any nano-filament and once with it. The largest difference between both curves occurs around the equilibrium Fermi level of the structure. In the second sub-plot, the quantum conductance computed with DFT+NEGF in the

linear theory approximation is compared with the experimental data of Ref. [23]. It has been discovered that each time a single atom is added to the growing nano-filament, its conductance abruptly changes from one plateau to another. However, the steps are not equal to the conductance quantum G_0=7.748e-5 S, but to a fraction of it since electrons must tunnel through the filament head to reach the opposite metallic plate. Due to the extremely narrow cross section of the filament and the resulting high current densities self-heating effects are expected to be important. They have not been studied so far because of the difficulty to properly include Eq. (5) into a DFT+NEGF solver and combine it with phonon transport.

IV. Conclusion

This paper has presented three applications of atomistic device simulations where the modeling approach has been adapted to the characteristics of each studied configuration. Generally, it can be stated that in well-known and -parameterized materials empirical tight-binding models offer a satisfactory level of accuracy and enable the inclusion of dissipative scattering mechanisms. In cases where a small and representative unit cell can be identified from the device structure a plane-wave DFT calculation combined with a unitary transformation into a maximally localized Wannier function basis appears as a very convenient solution. Going beyond the ballistic limit of transport is possible in this framework too. Finally, in complex geometries with metals, unconventional materials, or complex heterojunctions it is recommended to adopt a DFT+NEGF solver, which is very often restricted to ballistic simulations. Including electron-phonon scattering in large systems treated with DFT+NEGF still represents one of the greatest challenges in the field, together with modeling electron-electron interactions or coupled electron-phonon-photon phenomena.

Acknowledgment

This work was supported by SNF Grant No. PP00P2_159314, by the European Research Council under Grant Agreement No 335684-E-MOBILE, by the EU FP7 DEEPEN project, and by a grant from the Swiss National Supercomputing Centre under Project No. s662.

References

[1] S. Datta, "Electronic Transport in Mesoscopic Systems", Cambridge University Press, Cambridge (1995).

[2] N. Mingo and L. Yang, "Phonon transport in nanowires coated with an amorphous material: An atomistic Greens function approach", Phys. Rev. B 68, 245406 (2003).

[3] C. S. Lent and D. J. Kirkner, "The quantum transmitting boundary method", J. Appl. Phys. 67, 6353 (1990).

[4] M. Luisier et al., "Atomistic Simulation of Nanowires in the $sp^3d^5s^*$ Tight-Binding Formalism: from Boundary Conditions to Strain Calculations, Phys. Rev. B, **74**, 205323 (2006).

[5] M. Luisier and G. Klimeck, "Atomistic full-band simulations of silicon nanowire transistors: Effects of electron-phonon scattering", Phys. Rev. B 80, 155430 (2009).

[6] R. Rhyner and M. Luisier, "Atomistic modeling of coupled electron-phonon transport in nanowire transistors", Phys. Rev. B 89, 235311 (2014).

[7] R. Lake, G. Klimeck, R. C. Bowen, and D. Jovanovic, "Single and multiband modeling of quantum electron transport through layered semiconductor devices", J. Appl. Phys. 81, 7845 (1997).

[8] J. C. Slater and G. F. Koster, "Simplified LCAO Method for the Periodic Potential Problem", Phys. Rev. 94, 1498 (1954).

[9] T. B. Boykin, G. Klimeck, and F. Oyafuso, "Valence band effective-mass expressions in the $sp^3d^5s^*$ empirical tight-binding model applied to a Si and Ge parametrization", Phys. Rev. B 69, 115201 (2004).

[10] R. Rhyner and M. Luisier, "Phonon-limited low-field mobility in silicon: Quantum transport vs. linearized Boltzmann Transport Equation", J. Appl. Phys. 114, 223708 (2013).

[11] M. Luisier, "Atomistic modeling of anharmonic phonon-phonon scattering in nanowires", Phys. Rev. B 86, 245407 (2012).

[12] B. Radisavljevic, A. Radenovic, J. Brivio, V. Giacometti, and A. Kis, "Single-layer MoS_2 transistors", Nat. Nanotech. 6, 147 (2011).

[13] Y. Yoon et al., "How Good Can Monolayer MoS_2 Transistors Be?", Nano Letters 11, pp 3768-3773 (2011).

[14] N. Marzari and D. Vanderbilt, "Maximally localized generalized Wannier functions for composite energy bands", Phys. Rev. B 56, 12847 (1997).

[15] W. Kohn and L. J. Sham, "Self-Consistent Equations Including Exchange and Correlation Effects", Phys. Rev. 140, A1133 (1965).

[16] G. Kresse and J. Furthmüller, "Efficiency of ab-initio total energy calculations for metals and semiconductors using a plane-wave basis set", Comput. Mat. Sci. 6, 15 (1996).

[17] P. Giannozzi et al., "QUANTUM ESPRESSO: a modular and open-source software project for quantum simulations of materials", J. Phys.: Cond. Matt. 39, 395502 (2009).

[18] A. A. Mostofi, J. R. Yates, Y.-S. Lee, I. Souza, D. Vanderbilt, and N. Marzari, "Wannier90: A Tool for Obtaining Maximally-Localised Wannier Functions", Comput. Phys. Commun. 178, 685 (2008).

[19] J. P. Perdew, K. Burke, and M. Ernzerhof, "Generalized Gradient Approximation Made Simple", Phys. Rev. Lett. 77, 3865 (1997).

[20] A. Szabó, R. Rhyner, and M. Luisier, "*Ab initio* simulation of single- and few-layer MoS_2 transistors: Effect of electron-phonon scattering, Phys. Rev. B 92, 035435 (2015).

[21] A. Togo, F. Oba, and I. Tanaka, "First-principles calculations of the ferroelastic transition between rutile-type and $CaCl_2$-type SiO_2 at high pressures", Phys. Rev. B 78, 134106 (2008).

[22] L. O. Chua, "Memristor - The Missing Circuit Element", IEEE Trans. Circ. Theory 18, 507 (1971).

[23] A. Emboras et al., "Atomic Scale Plasmonic Switch", Nano Lett. **16**, 709-714 (2016).

[24] M. Brandbyge, J. L. Mozos, P. Ordejon, J. Taylor, and K. Stokbro, "Density-functional method for nonequilibrium electron transport", Phys. Rev. B 74, 165401 (2002).

[25] J. Izquierdo et al., "Systematic *ab initio* study of the electronic and magnetic properties of different pure and mixed iron systems", Phys. Rev. B 61, 13639 (2000).

[26] J. VandeVondele et al., "Quickstep: fast and accurate density functional calculations using a mixed Gaussian and plane waves approach", Comp. Phys. Comm. **167**, 103-128 (2005).

[27] M. Calderara et al., "Pushing back the limit of ab-initio quantum transport simulations on hybrid supercomputers", SC'15 Proceedings of the International Conference for High Performance Computing, Networking, Storage and Analysis, Article No. 3 (2015).